Published OnlineFirst July 27, 2010; DOI: 10.1158/0008-5472.CAN-10-1440

Cancer Research

Development of a Novel Tumor-Targeted Vascular Disrupting Agent Activated by Membrane-Type Matrix Metalloproteinases

Jennifer M. Atkinson[1], Robert A. Falconer[1], Dylan R. Edwards[2], Caroline J. Pennington[2], Catherine S. Siller[1], Steven D. Shnyder[1], Michael C. Bibby[1], Laurence H. Patterson[1], Paul M. Loadman[1], and Jason H. Gill[1]

Abstract

Vascular disrupting agents (VDA) offer a strategy to starve solid tumors of nutrients and oxygen concomitant with tumor shrinkage. Several VDAs have progressed into early clinical trials, but their therapeutic value seems to be compromised by systemic toxicity. In this report, we describe the design and characterization of a novel VDA, ICT2588, that is nontoxic until activated specifically in the tumor by membrane-type 1 matrix metalloproteinase (MT1-MMP). HT1080 cancer cells expressing MT1-MMP were selectively chemosensitive to ICT2588, whereas MCF7 cells that did not express MT1-MMP were nonresponsive. Preferential hydrolysis of ICT2588 to its active metabolite (ICT2552) was observed in tumor homogenates of HT1080 relative to MCF7 homogenates, mouse plasma, and liver homogenate. ICT2588 activation was inhibited by the MMP inhibitor ilomastat. In HT1080 tumor–bearing mice, ICT2588 administration resulted in the formation of the active metabolite, diminution of tumor vasculature, and hemorrhagic necrosis of the tumor. The antitumor activity of ICT2588 was superior to its active metabolite, exhibiting reduced toxicity, improved therapeutic index, enhanced pharmacodynamic effect, and greater efficacy. Coadministration of ICT2588 with doxorubicin resulted in a significant antitumor response (22.6 d growth delay), which was superior to the administration of ICT2588 or doxorubicin as a single agent, including complete tumor regressions. Our findings support the clinical development of ICT2588, which achieves selective VDA targeting based on MT-MMP activation in the tumor microenvironment. *Cancer Res; 70(17); 6902–12. ©2010 AACR.*

Introduction

Disruption of the vascular network within tumors is known to be an efficient chemotherapeutic strategy, with a number of vascular disrupting agents (VDA) currently undergoing clinical trials (1, 2). Several VDAs target the colchicine-binding site of tubulin, induce rapid conformational changes in tumor vasculature, blood vessel occlusion, and consequent tumor necrosis (1–4). The disruption of a single tumor blood vessel has the effect of starving and consequently killing the many tumor cells it supports, making this a very effective therapeutic strategy. However, the prevalence of cardiotoxicity, cardiac ischemia, and arrhythmias in clinical trials of systemically administered VDAs targeting the colchicine-binding site of tubulin suggests that their therapeutic value is compromised by intrinsic systemic toxicity (5–7). Strategies focused on improving the therapeutic index of these VDAs, reducing systemic exposure, and improving tumor selectivity and response are paramount.

Matrix metalloproteinases (MMP) comprise a family of 24 zinc-dependent endopeptidases with structural similarity and a pivotal role in tumorigenesis and tumor progression (8–10). Originally, it was believed that the MMPs functioned purely to break down the extracellular matrix to facilitate tumor invasion, a concept now shown to be too simplistic (9). In addition to extracellular matrix breakdown and tumor cell invasion, MMPs also play a major role in controlling tumor cell growth, migration, differentiation, and ultimately metastasis (8, 9). The MMP family comprises two groups, that is, the soluble and membrane-type MMPs (MT-MMPs), with the MT-MMPs further subclassified by their cell surface association, either by a transmembrane domain (MT1, 2, 3, and 5) or by a glycophosphatidylinositol anchor (MT4 and 6). Transmembrane MT-MMPs play a role in many tumorigenic processes, and their expression is elevated in a wide

Authors' Affiliations: [1]Institute of Cancer Therapeutics, School of Life Sciences, University of Bradford, Bradford, West Yorkshire, United Kingdom and [2]School of Biological Sciences, University of East Anglia, Norwich, United Kingdom

Note: Supplementary data for this article are available at Cancer Research Online (http://cancerres.aacrjournals.org/).

Current address for J.M. Atkinson: Department of Developmental Neurobiology, St. Jude Children's Research Hospital, Memphis, TN 38105.

Corresponding Authors: Jason H. Gill and Paul M. Loadman, Institute of Cancer Therapeutics, School of Life Sciences, University of Bradford, Bradford, West Yorkshire BD7 1DP, United Kingdom. Phone: 44-1274-233226; Fax: 44-1274-233234; E-mail: j.gill1@bradford.ac.uk and p.m.loadman@bradford.ac.uk.

doi: 10.1158/0008-5472.CAN-10-1440

Published OnlineFirst July 27, 2010; DOI: 10.1158/0008-5472.CAN-10-1440

range of tumors, including non–small cell lung cancer (11–15). MT1-MMP (also known as MMP-14), the prototypic and most widely studied member of this family, has a crucial role in tumorigenesis, particularly tumor cell dissemination and metastasis (15–18). For instance, induced expression of MT1-MMP into null or nonmalignant cells renders the cells capable of invasion, and knockdown of MT1-MMP inhibits cell invasion and tumor progression (19–23). A crucial role for MT1-MMP in tumor angiogenesis has been reported by several *in vitro* and *in vivo* studies (12, 24–26). The therapeutic potential of this is illustrated by MT1-MMP–selective antibody inhibition of angiogenesis and tumor progression (25). The pivotal role for MT1-MMP in tumor expansion and progression, its elevated expression in a wide range of tumor types and its unique localization tethered to the cell surface, strongly support its potential as a target for therapeutic exploitation in cancer.

Several successful approaches for targeting chemotherapy directly to malignant tissue have emerged, including antigen targeting, antibody- or gene-directed enzyme prodrug therapy, and tumor enzyme–activated chemotherapy (27). In particular, the exploitation of enzymes elevated selectively in the tumor microenvironment to convert an inactive drug into its active chemotherapeutic metabolite has shown significant promise, as exemplified by the bioreductive drug AQ4N (Banoxantrone; refs. 28, 29) and the clinically used agent capecitabine (Xeloda; refs. 27, 30). Consequently, a significant effort has been focused on the identification of suitable tumor enzymology and the development of therapeutics directed against these targets, including proteolytic enzymes of the tumor degradome (31). In this regard, a potential strategy to improve the therapeutic index of VDAs is to selectively release an active VDA from an inactive form within the tumor microenvironment, such as by using the increased activity of MMPs (31).

In this study, we have designed and developed a novel agent (ICT2588) that is selectively metabolized by MT-MMPs, particularly MT1-MMP, to release an active VDA, azademethylcolchicine (ICT2552). The activation of this agent (ICT2588) selectively in the tumor, coupled with negligible/undetectable levels of the active azademethylcolchicine (ICT2552) in normal tissues *in vivo*, led to a significant antitumor effect with a greater therapeutic index. Furthermore, coadministration of ICT2588 with the chemotherapeutic agent doxorubicin resulted in a significantly enhanced antitumor effect and tumor cures in preclinical studies.

Materials and Methods

Cell culture

The human fibrosarcoma (HT1080; ATCC CCL-121) and breast carcinoma (MCF7; ATCC HTB-22) cell lines were obtained from American Type Culture Collection and were authenticated both morphologically and by short tandem repeat analysis. Cell lines were cultured as monolayers in RPMI 1640 supplemented with 10% (v/v) fetal bovine serum, 1 mmol/L of sodium pyruvate, and 2 mmol/L of L-glutamine. All cell lines were used at a low passage in our laboratory for a maximum of 6 months postresuscitation and were tested regularly to confirm lack of *Mycoplasma* infection.

Animals

Female BALB/c immunodeficient nude mice (Harlan Blackthorne) were housed in an air-conditioned room with regular alternating cycles of light and darkness and received Harlan 2018 diet and water *ad libitum*. The facilities were approved by the Home Office and met all current regulations and standards of the United Kingdom. The mice were used between the ages of 6 and 8 weeks in accordance with institutional guidelines, and all procedures were carried out under a U.K. Home Office Project License, following U.K. Coordinating Committee on Cancer Research guidelines (32).

Mice were implanted s.c. with 2 to 3 mm^3 fragments of HT1080 or MCF7 tumor xenografts. Resultant tumors were removed, snap-frozen in liquid nitrogen, and stored at –70°C.

Quantification of MMP expression by real-time reverse transcription-PCR

Assessment of MMP gene expression as determined by quantitative reverse transcription-PCR was performed as previously described (33). The 18S rRNA gene was used as an endogenous control, using previously validated procedures (34). All primers and fluorogenic probe nucleotide sequences were previously shown to be MMP gene–specific (33, 34). The C_T (cycle at which amplification entered the exponential phase) was used as an indicator of the level of target RNA in each tissue, that is, a lower C_T indicated a higher quantity of target RNA.

Immunoblotting

Cells were lysed on ice with extraction buffer, containing 50 mmol/L of Tris-HCl (pH 7.6), 1.5 mmol/L of NaCl, 0.5 mmol/L of $CaCl_2$, 1 μmol/L of ZnCl, 0.01% Brij 35, and 0.25% Triton X-100 for 15 minutes. For xenograft tumors, tissue was weighed, incubated on ice in extraction buffer for 15 minutes, homogenized, and incubated for a further 15 minutes on ice. The resulting protein extract was collected via centrifugation at 2,000 × *g* for 10 minutes at 4°C. Equal amounts of proteins (representing 1×10^5 cells or 0.1 mg xenograft tissue) were resolved by 10% SDS-PAGE and blotted onto Hybond-P membrane (Amersham, United Kingdom). Nonspecific antibody binding was blocked via incubation in 5% enhanced chemiluminescence blocking reagent (Amersham). The blot was probed with a monoclonal antibody to MT1-MMP (MAB3328; Chemicon International) overnight at 4°C followed by a rabbit anti-mouse horseradish peroxidase–conjugated antibody (Dako). Antibody reactivity was detected by chemiluminescence using ECL-Plus (Amersham).

Synthesis of MT-MMP targeted compound

The MT-MMP–targeted agent, ICT2588 (Fig. 2A), was synthesized as a COOH-terminal– and NH_2-terminal–modified peptide conjugate of azademethylcolchicine (ICT2552) using a combinatorial of solution and solid phase chemistries, as developed in house (35). Compound purity and identity

Published OnlineFirst July 27, 2010; DOI: 10.1158/0008-5472.CAN-10-1440

was shown by high-performance liquid chromatography and mass spectrometry (Supplementary Fig. S1).

Cell chemosensitivity

In vitro chemosensitivity of HT1080 and MCF7 cells to the agents was determined using the 3-(4,5-dimethylthiazol-2-yl)-2,5-diphenyltetrazolium bromide assay, described elsewhere (36). Cells were exposed to ICT2588 (2.4 nmol/L to 5 μmol/L), its authentic metabolite, ICT2552 (0.1 nmol/L to 5 μmol/L), or solvent (DMSO). Solvent concentrations did not exceed 0.1% and were not cytotoxic. Chemosensitivity was assessed following either 24 or 96 hours of agent exposure, with cell survival determined 96 hours posttreatment. Survival curves were obtained and IC_{50} values calculated.

Immunocytochemical analysis of microtubule disruption

Assessment of microtubule disruption induced by ICT2588 and ICT2552 in HT1080 and MCF7 cells was performed using previously described methodologies (37). ICT2588 or its authentic metabolite, ICT2552, were tested at the IC_{50} concentration identified for HT1080 [as determined by 3-(4,5-dimethylthiazol-2-yl)-2,5-diphenyltetrazolium bromide assay] and at one-tenth this dose. After 24 hours of agent exposure, tubulin disruption was assessed by α-tubulin fluorescence immunocytochemistry and visualized by confocal microscopy.

ICT2588 metabolism in tissues *ex vivo*

Cell pellets and xenograft tumors were homogenized in MMP activity buffer [50 mmol/L Tris-HCl (pH 7.6), 1.5 mmol/L NaCl, 0.5 mmol/L $CaCl_2$, 1 μmol/L ZnCl, and 0.01% v/v Brij-35] and the resultant supernatants collected by centrifugation. Supernatants (equivalent to 100 mg tissue/mL) were then assayed for their ability to activate ICT2588 (final concentration, 20 μmol/L). Reaction aliquots were removed over a 120-minute period, proteins precipitated using acetonitrile, and agent and metabolites analyzed by liquid chromatography-mass spectrometry (LC-MS). Detection was performed on a Waters Alliance system using a photodiode array detector, and a Micromass ZMD Mass Spectrometer connected in series. Agent and metabolites were separated on a RPB reversed-phase high-performance liquid chromatography column (HiChrom) using a mobile phase of acetonitrile/water/0.05% trifluoroacetic acid, with a gradient from 22.5% to 50% acetonitrile over 30 minutes at 1.2 mL/min. ICT2588 was quantified using absorption measurement at 360 nm. Metabolic intermediates were detected as singularly and doubly charged ions and identified by mass spectrometry.

MMP selectivity was shown by the ability of recombinant MMPs (200 ng) to activate ICT2588 (20 μmol/L) by incubation at 37°C in MMP activity buffer. In parallel, MMPs were incubated with a control substrate to verify proteolytic activity. Activation was assessed by recombinant human MT1-, MT2-, MT3-, MT5-MMP, and MMP-9 (Chemicon) and MMP-1, -2, -10, -12, and -13 (R&D Systems; detailed in Supplementary Fig. S2). Aliquots of the reaction (20 μL) were removed at intervals up to 9 hours and analyzed by LC-MS.

To confirm MMP involvement in the metabolism of ICT2588, homogenates of HT1080 xenografts were coincubated with either ilomastat (GM6001; Chemicon; ref. 38), a broad-spectrum MMP inhibitor, or CTT (Biomol; ref. 39), a selective MMP-2/MMP-9 inhibitor. These homogenates were assayed for their ability to activate ICT2588 in the presence of inhibitor, as described above.

Pharmacokinetic analyses

Distribution, activation, and metabolism of ICT2588 and ICT2552 were evaluated in mice bearing HT1080 tumors. Mice were injected i.p. with either ICT2588 (150 mg/kg), ICT2552 (10.2 mg/kg), or solvent (10% DMSO/arachis oil). Tumors, blood, and normal tissues (liver, kidney, lung, heart, and spleen) were collected at defined times posttreatment. Blood was centrifuged at 5,000 × *g* for 10 minutes, and the resulting plasma diluted 1:5 into methanol. Tissue samples were immediately frozen in liquid nitrogen prior to homogenization in ice-cold methanol. Following centrifugation, concentrations of agent and metabolites were determined in the resultant supernatants by LC-MS. Calibration samples were established using agent-free plasma and tissues.

To differentiate the activated metabolite produced by proteolysis of ICT2588 from that of the nonconjugated agent (azademethylcolchicine), these are termed $ICT2552^{act}$ and ICT2552, respectively.

Assessment of vascular shutdown and induction of tumor necrosis

The degree of functional tumor vasculature and proportion of hemorrhagic necrosis was assessed 24 hours following i.p. administration of ICT2552 (10.2 mg/kg), ICT2588 (150 mg/kg), or solvent (10% DMSO/arachis oil) to mice bearing HT1080 tumors, using methodologies described and detailed previously (37, 40, 41)

Antitumor activity

Mice bearing HT1080 tumors of ~32 mm^3 were randomized into groups receiving either ICT2588 (37.5, 50, 62.5, or 75 mg/kg) or the molar equivalent of its authentic metabolite (ICT2552; 7.5, 10, 12.5, or 15 mg/kg) via i.p. administration. Tumor volume (measured by calipers) and animal body weight were recorded daily for up to 64 days. Tumor volumes were calculated using the formula: $(a^2 \times b)/2$ (a being the smaller and b the larger dimension of the tumor), and normalized to the respective volume on day 0. Mann-Whitney U tests were performed to determine the statistical significance of any differences in growth rate (based on tumor volume doubling time) between control and treated groups, and between the different compounds.

For combination studies with doxorubicin, ICT2588 was administered i.p. at 75 mg/kg, whereas doxorubicin was administered i.v. at 5 mg/kg. The study involved five treatment groups: ICT2588 alone, doxorubicin alone, doxorubicin administered 20 minutes prior to ICT2588, doxorubicin administered 6 hours after ICT2588, or doxorubicin administered 24 hours after ICT2588. Tumor measurements were conducted as described above.

Published OnlineFirst July 27, 2010; DOI: 10.1158/0008-5472.CAN-10-1440

A

Origin	Cell line	MMP-1	MMP-2	MMP-3	MMP-7	MMP-8	MMP-9	MMP-10	MMP-11	MMP-12	MMP-13	MT1-MMP	MT2-MMP	MT3-MMP	MT4-MMP	MMP-19	MMP-20	MMP-21	MMP-23	MT5-MMP	MT6-MMP	MMP-26	MMP-28
Fibrosarcoma	HT1080																						
Breast	MCF7																						
	MDA-231																						
Colon	HT29																						
	BE																						
	HCT116																						
	COLO205																						
	DLD1																						
Lung	A549																						
	H661																						
	BEAS2B																						
	H460																						
Prostate	PC3																						
	LNCAP																						

B

Origin	Xenograft	MMP-1	MMP-2	MMP-3	MMP-7	MMP-8	MMP-9	MMP-10	MMP-11	MMP-12	MMP-13	MT1-MMP	MT2-MMP	MT3-MMP	MT4-MMP	MMP-19	MMP-20	MMP-21	MMP-23	MT5-MMP	MT6-MMP	MMP-26	MMP-28
Fibrosarcoma	**HT1080**																						
Breast	**MCF7**																						
Colon	**BE**																						
	HCT116																						
	COLO205																						
	DLD1																						
	HT29																						
Lung	**A549**																						
	H460																						
Prostate	**PC3**																						

C

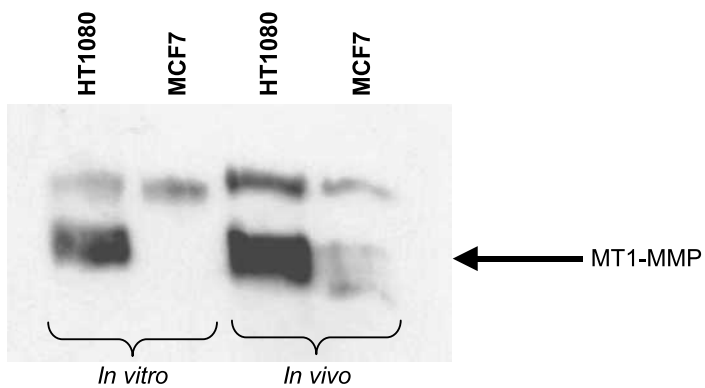

Figure 1. MT-MMPs are elevated in human preclinical tumor models. Expression of MMP mRNA in human cell lines grown *in vitro* (A) and as xenografts *in vivo* (B) as measured by quantitative reverse transcription-PCR. Expression values were measured after normalization to 18S-rRNA and are gene-specific. Classification of expression levels was determined from the C_T of each gene as either very high ($C_T \leq 25$), high ($C_T = 26–30$), moderate ($C_T = 31–35$), low ($C_T = 36–39$), or not detected ($C_T = 40$); see key for color scheme. C, immunoblot of MT1-MMP protein expression in HT1080 and MCF7 tumor models. Key for quantitative reverse transcription-PCR expression: □, negative; ■, low; ■, moderate; ■, high; ■, very high expression.

Published OnlineFirst July 27, 2010; DOI: 10.1158/0008-5472.CAN-10-1440

Results

MMPs and MT-MMPs are differentially expressed in human preclinical tumor models

The expression profile of MMPs in human preclinical tumor models reported in the literature is incomplete. Using human cell lines and associated xenograft models representing a range of tumor types, we assessed the expression of 22 MMPs using quantitative reverse transcription-PCR. A diverse profile of MMP expression in both human tumor cell lines (Fig. 1A) and the corresponding *in vivo* xenograft models (Fig. 1B) was observed. High expression levels of MT1-MMP were observed in the majority of tumor models analyzed, with extremes being the fibrosarcoma model HT1080 (very high levels; $C_T \leq 25$) and the breast carcinoma cell line MCF7 (undetectable MT1-MMP mRNA; $C_T = 40$). This strongly supports the presence of active MT1-MMP, as previously reported by our group (33). The differential was further confirmed at the protein level in cell lines by Western blotting (Fig. 1C), in agreement with previous studies (25, 26). In contrast with cell lines grown *in vitro*, a weak band corresponding to MT1-MMP protein was observed in *ex vivo* MCF7 tumor homogenates (Fig. 1C).

Differential activation of ICT2588 in human tumor models *in vitro*

HT1080 and MCF7 cells were used to assess the activation and cytotoxicity of our azademethylcolchicine-peptide conjugate (ICT2588) *in vitro*. HT1080 cells (MT1-MMP positive) were at least 10-fold more chemosensitive to ICT2588 than MCF7 cells (MT1-MMP negative) *in vitro* (Table 1). This is in contrast with exposure of the cells to the authentic metabolite, ICT2552, which was equally cytotoxic to HT1080 and MCF7 cells (Table 1). These differentials in cytotoxicity were reflected pharmacodynamically by the induction of tubulin disruption in these cell lines. ICT2552 induced tubulin foci and morphologic changes indicative of tubulin disruption in both HT1080 and MCF7 cells *in vitro*. In contrast, the peptide-conjugated agent (ICT2588) induced these changes in the HT1080 cell line but not the MCF7 cells *in vitro* (data not shown).

The lack of activity of ICT2588 against MCF7 and the lack of observable intracellular fluorescence following treatment also supported the concept that the peptide-conjugated agent, ICT2588, was inactivated and could not enter cells, thereby requiring activation by extracellular proteolysis.

Table 1. Differential chemosensitivity of the peptide-conjugate (ICT2588) and active metabolite (ICT2552) against MT1-MMP–positive (HT1080) and –negative (MCF7) cell lines *in vitro*

	Compound	HT1080 IC_{50} (nmol/L)	MCF7 IC_{50} (nmol/L)
24 h	ICT2588	*522 ± 76*	>5,000
	ICT2552	*36 ± 5*	*64 ± 28*
96 h	ICT2588	*176 ± 39*	>5,000
	ICT2552	*31 ± 1.3*	*63 ± 20*

NOTE: Values are reported as IC_{50}. Values represent the mean for three independent experiments ± SD. Values in italics indicate a positive cytotoxic response.

MT-MMP–selective activation of ICT2588

A panel of recombinant MMPs, representing the different MMP subclasses were used to evaluate the selectivity and site of proteolytic cleavage *in vitro*. The type I MT-MMPs [MT1-$^{(MMP-14)}$, MT2-$^{(MMP-15)}$, MT3-$^{(MMP-16)}$, and MT5-$^{(MMP-24)}$] hydrolyzed the glycine-homophenylalanine bond of ICT2588 (Fig. 2A; Supplementary Fig. S2). The secreted MMP-2, which is regulated by MT1-MMP (42), was also observed to activate ICT2588 through cleavage of the homophenylalanine-tyrosine bond (Fig. 2A). In contrast, activation of ICT2588 was not observed by the other recombinant-secreted MMPs evaluated.

Metabolism of ICT2588 in tumor but not normal tissues

In order for ICT2588 to be a viable therapeutic strategy, it must show activation in tumor tissue, systemic stability, and limited activation in non-diseased tissue. Metabolism of ICT2588 and formation of its authentic metabolite, ICT2552^{act}, were studied *ex vivo* using HT1080 and MCF7 human tumor xenograft homogenates and murine plasma and tissues. Rapid metabolism of ICT2588 was observed in the HT1080 xenograft homogenate ($t_{1/2}$ = 4.4 min). In comparison, ICT2588 was relatively stable in MCF7 xenograft homogenate ($t_{1/2}$ = 33.1 min), murine liver ($t_{1/2}$ = 22.0 min), and murine blood plasma ($t_{1/2}$ > 40 min; Fig. 2B).

Metabolism of ICT2588 in HT1080 homogenates resulted in the rapid production of active azademethylcolchicine, with no detectable peptide-conjugated metabolites of ICT2588. To observe these metabolites, homogenates required >500-fold dilution or the reaction was conducted at 4°C (date not shown). The rapid metabolism of these intermediates to the active agent was confirmed using the chemically synthesized peptide-conjugated metabolites.

The involvement of MMPs was assessed by determining the degree of agent activation by HT1080 homogenates in the presence of the MMP inhibitor ilomastat (GM6001; ref. 38) and the MMP-2/MMP-9–selective inhibitor CTT (39). Ilomastat resulted in a dose-dependent decrease in metabolism of ICT2588 by HT1080 (Fig. 2C). In contrast, no significant inhibition of ICT2588 activation was observed in the presence of CTT (data not shown).

Tissue distribution of ICT2588 and tumor-selective activation *in vivo*

Following ICT2588 administration, ICT2588 and its corresponding metabolites were measured. The activated metabolite produced by proteolysis of ICT2588 is termed ICT2552^{act}. The pharmacokinetic profile of ICT2588 (Fig. 3:

Published OnlineFirst July 27, 2010; DOI: 10.1158/0008-5472.CAN-10-1440

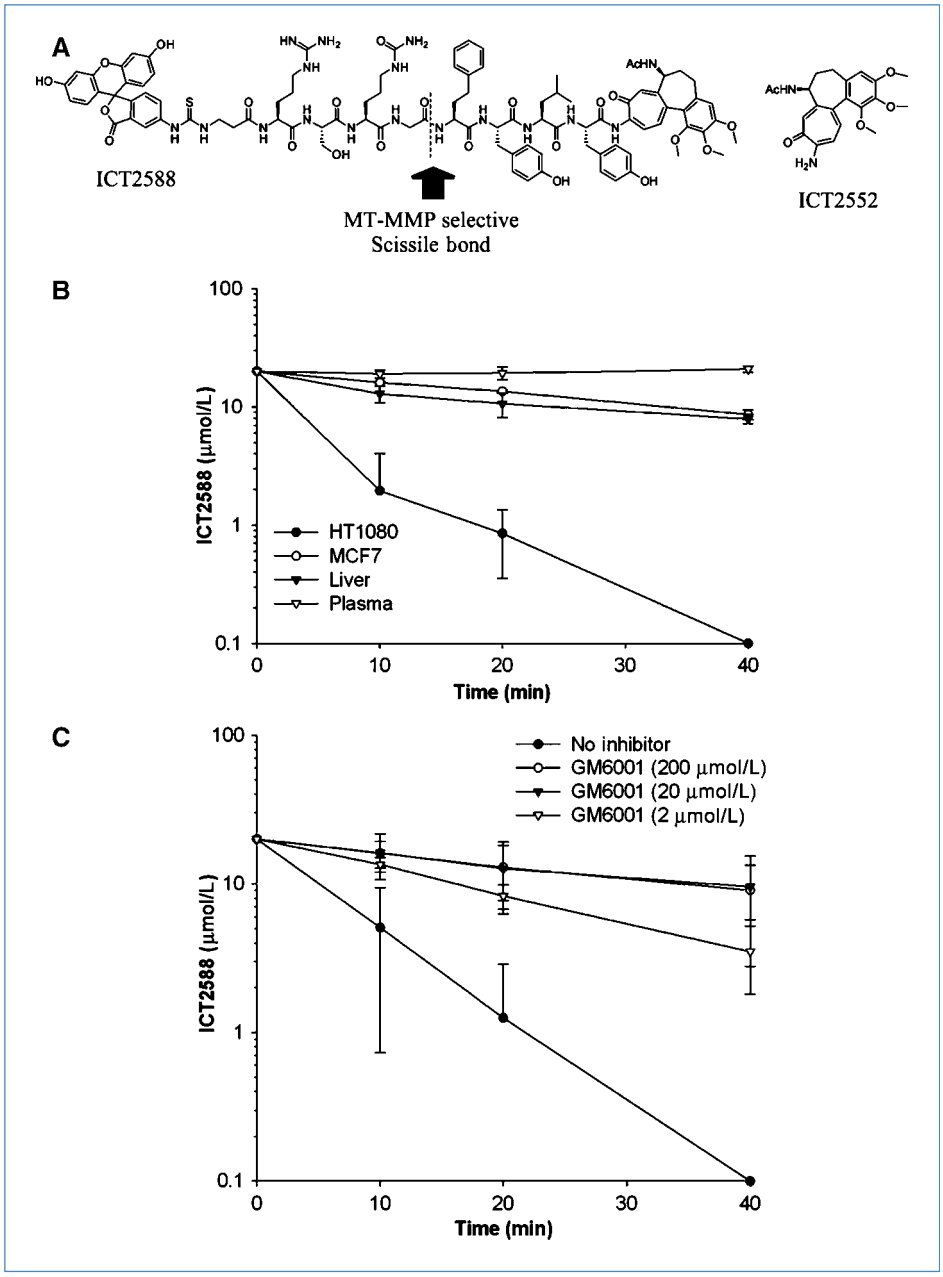

Figure 2. ICT2588 is selectively activated by MMPs. A, structure of ICT2588 and ICT2552, indicating the MT-MMP–selective scissile bond. B, metabolism of ICT2588 by HT1080 and MCF7 tumors relative to mouse liver and mouse plasma. Metabolites detected by LC-MS and expressed as concentration of ICT2588 remaining. C, metabolism of ICT2588 in the presence of a pan-MMP inhibitor, ilomastat (GM-6001). Points, mean of three independent experiments; bars, SD.

Supplementary Fig. S3) shows extensive distribution of the parent agent with accumulation in the tumor tissue with time. Furthermore, a differential in ICT2552^{act} concentration in tumor compared with normal tissues was observed (Fig. 3B; Supplementary Fig. S3). All throughout the experiment, levels of ICT2552^{act} were below detectable levels in plasma and heart (Fig. 3C; Supplementary Fig. S3). In all tissues investigated, concentrations of activated agent (ICT2552^{act}) following ICT2588 administration were at least 50% lower in mouse organs relative to tumor tissue. After 6 hours, ICT2552^{act} was still present in tumor tissue but was below detectable levels in normal tissues investigated (Fig. 3C; Supplementary Fig. S3). By way of comparison, ICT2552 (as a nonconjugated agent) was widely distributed throughout the mice following i.p. administration, with the liver being representative of all normal mouse tissues (Supplementary Fig. S3). At 4 hours postadministration, the concentrations of ICT2552 were not significantly different between tumor and liver tissue, but concentrations were below the level of detection in plasma (Supplementary Fig. S3).

Induction of tumor vascular collapse and hemorrhagic necrosis following ICT2588 treatment *in vivo*

Administration of ICT2588 to HT1080 tumor–bearing mice resulted in a 90% decrease in the level of functional tumor vasculature (Fig. 4A). This effect was comparable to that

Published OnlineFirst July 27, 2010; DOI: 10.1158/0008-5472.CAN-10-1440

observed following administration of ICT2552 at an equimolar concentration (80% reduction; Fig. 4A). This result is consistent with the conversion of the peptide-conjugated agent, ICT2588, to ICT2552^{act} within the tumor *in vivo* (Fig. 4A). Concurrent to the induction of vascular damage within the tumor by ICT2588 was the 3-fold increase in hemorrhagic necrosis (Fig. 4B) as well as a rim of viable tumor cells, consistent with other VDA therapeutics (Fig. 4B).

Antitumor activity of ICT2588

HT1080 tumor–bearing mice were treated with the MT1-MMP–targeted agent, ICT2588 (37.5, 50, 62.5, and 75 mg/kg) or the nonconjugated agent, ICT2552, at equimolar doses (7.5, 10, 12.5, and 15 mg/kg), and tumor growth compared with vehicle-treated controls. ICT2588 resulted in a significant antitumor response, with growth delays of between 2.0 and 5.6 days ($P < 0.01$; Fig. 5A); one mouse in the 62.5 mg/kg ICT2588 group showed a complete tumor remission. In contrast, ICT2552 at equimolar doses produced a significantly lower antitumor response (Fig. 5B). At all doses used, administration of ICT2588 led to no significant loss in mouse body weight (maximum of 6%; data not shown).

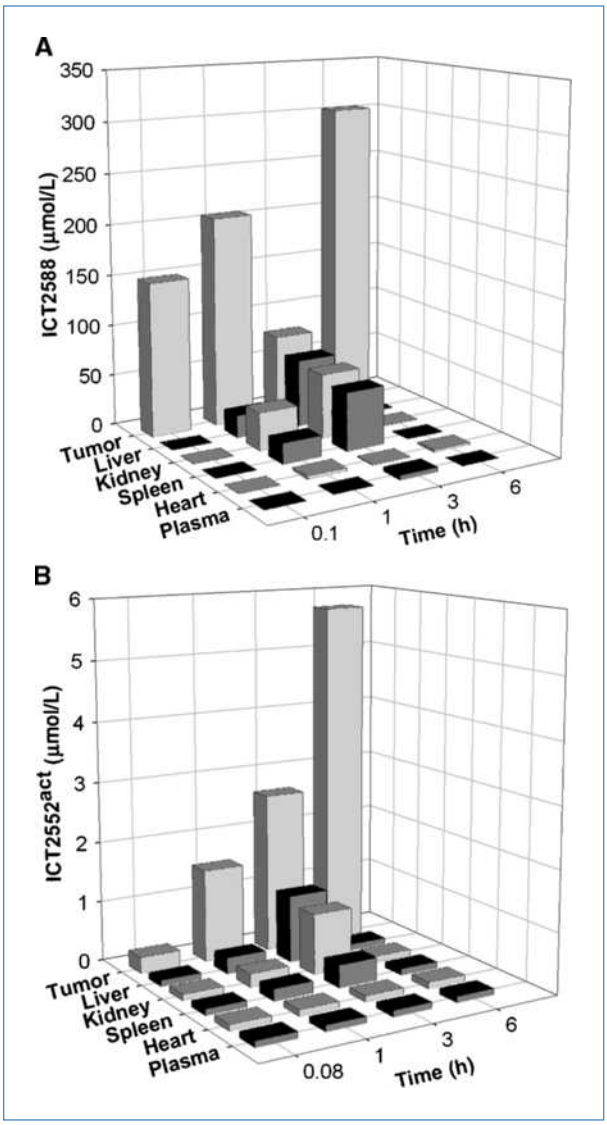

Figure 3. Pharmacokinetic analysis of ICT2588 following i.p. administration to HT1080 tumor–bearing mice. Analysis by LC-MS of (A) ICT2588 and (B) the authentic metabolite produced from hydrolysis of ICT2588 (ICT2552^{act}). Columns, mean of three mice; bars, SD.

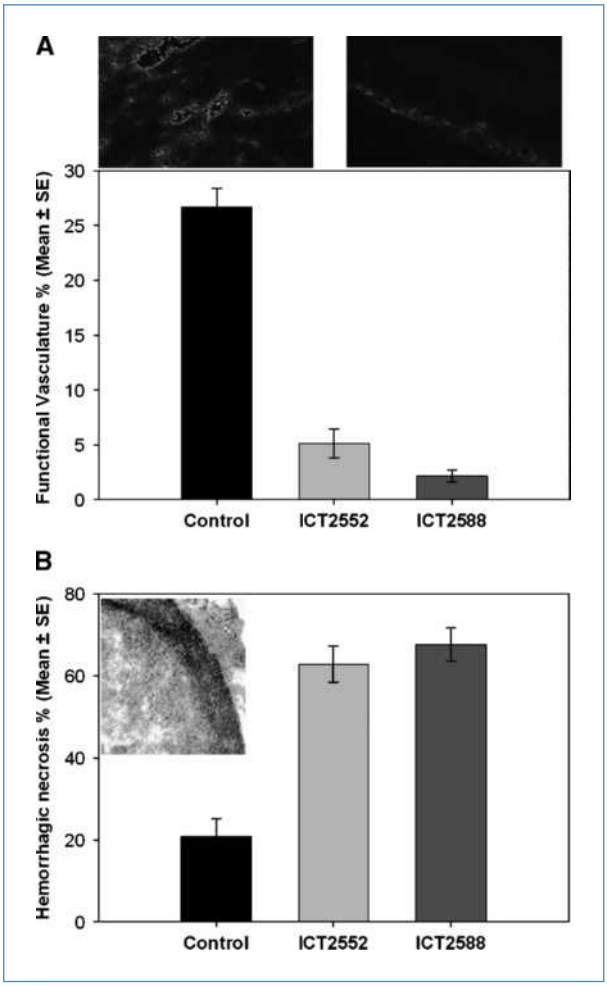

Figure 4. Induction of tumor vascular disruption and hemorrhagic necrosis by ICT2588 *in vivo*. Mice bearing HT1080 tumors were treated with ICT2588 or ICT2552 and assessed for functional vasculature (A) and hemorrhagic necrosis (B) 24 h posttreatment. Columns, mean from three mice; bars, SE. A, images show loss of functional tumor vasculature (as described previously; see refs. 37, 40, 41). B, images show persistence of a viable tumor rim.

Coadministration of ICT2588 with doxorubicin

Combination therapy of ICT2588 and doxorubicin in mice bearing HT1080 tumors produced a significant tumor response in all treatment groups relative to controls, ICT2588 or doxorubicin as a single agent. Administration of ICT2588 6 hours prior to doxorubicin (14-d growth delay) showed no

Published OnlineFirst July 27, 2010; DOI: 10.1158/0008-5472.CAN-10-1440

significant difference in the antitumor activity observed compared with coadministration of both agents simultaneously (19-d growth delay). However, administration of doxorubicin to mice with established ICT2588-induced vascular collapse (24 h) resulted in a significantly greater effect than dosing each agent alone and results in complete tumor remission or cure in the majority (four of seven) of treated mice (Fig. 5C). This result was obtained using ICT2588 and doxorubicin at 50% and 30% of their maximum deliverable doses, respectively.

Discussion

Disruption of the vascular supply to tumors is recognized as an effective therapeutic strategy (1, 2). Several colchicine-based VDAs have shown preclinical efficacy, but none have yet progressed through clinical trials. One reason for the lack of clinical progression of these VDAs is the prevalence of off-target effects on the cardiovascular system (2, 5, 6). A strategy to improve tumor selectivity with attendant diminution of systemic toxicity, and hence, improved therapeutic index

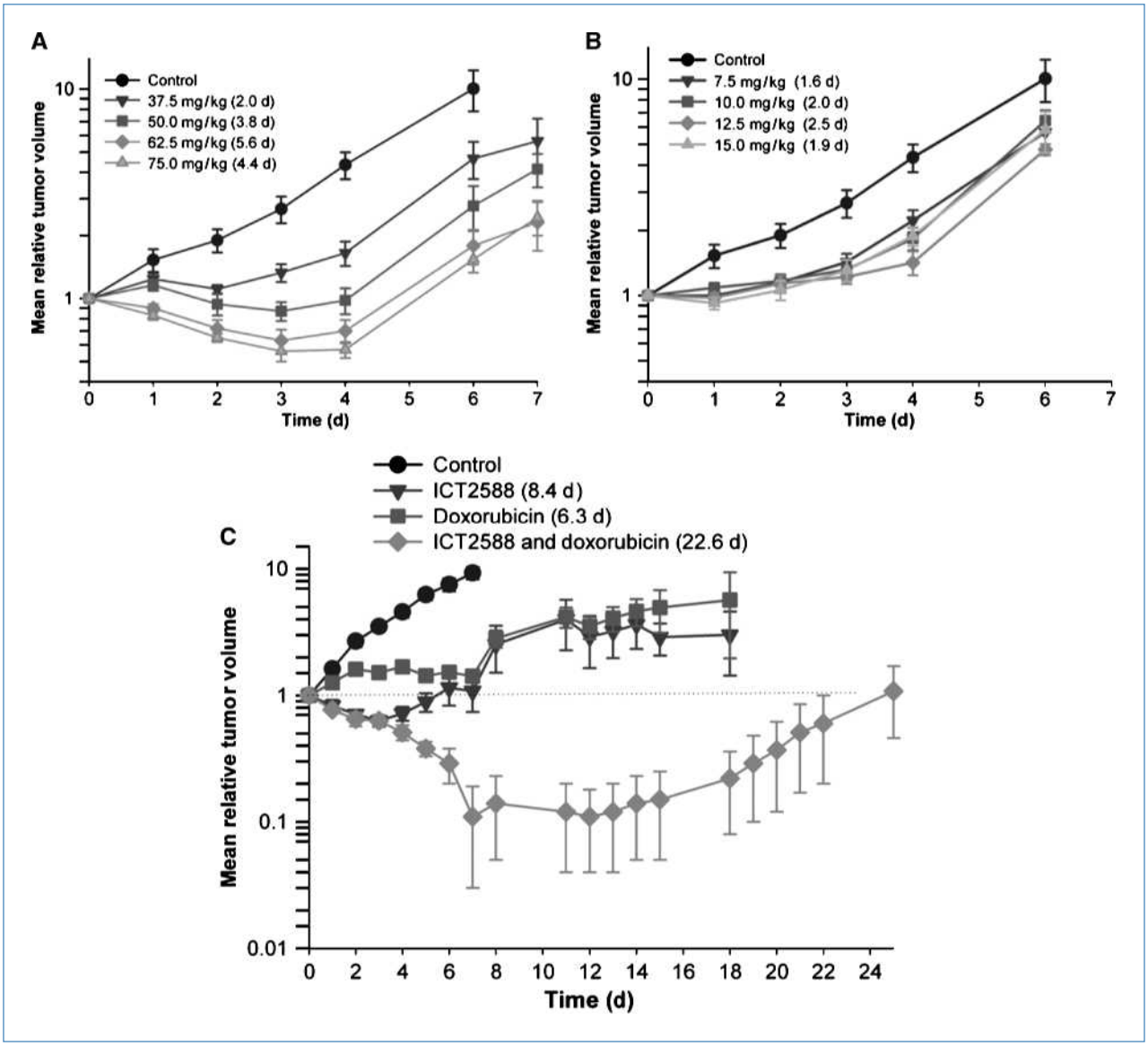

Figure 5. A, ICT2588 (peptide conjugate) induces a significantly greater inhibition of HT1080 tumor growth compared with (B) the authentic metabolite (ICT2552) at equimolar concentrations. Mice were treated with a single i.p. dose of ICT2588 (A) or ICT2552 (B) and tumor size determined daily (*, one animal in the ICT2588 62.5 mg/kg treatment group showed complete tumor remission). C, combination of ICT2588 with doxorubicin resulted in significantly greater antitumor potency relative to single-agent doxorubicin or ICT2588 administration. Mice were administered 75 mg/kg of ICT2588 (i.p.) 24 h prior to 5 mg/kg of doxorubicin (i.v.) and tumor size determined daily (C). Four out of eight mice showed complete tumor remission with the coadministration schedule; therefore, results in this group are the summary of four remaining mice. The tumor growth delay is defined as the time taken for doubling of tumor volume relative to control, denoted in parentheses in the key for each figure panel.

Published OnlineFirst July 27, 2010; DOI: 10.1158/0008-5472.CAN-10-1440

is an attractive approach to the development of VDAs. Consequently, we have preclinically designed and developed ICT2588 as a novel approach to the selective delivery of a VDA to be activated by MT-MMP endopeptidase in the tumor microenvironment.

Elevated expression of the class-I transmembrane MMPs, particularly MT1-MMP, was shown in a large number of tumor types across a panel of preclinical tumor models. Increased proteolytic activity in these tumors is supported by our previous study which showed a direct relationship between MT1-MMP mRNA expression and enzyme activity (33). Previous studies have also shown a correlation between MT1-MMP expression and malignancy of different tumor types (14, 15, 25). The detection of low levels of MT1-MMP protein in MCF7 xenografts (in contrast with MCF7 cells *in vitro*) indicates that MT1-MMP is also present in murine tumor stroma (18, 43) and tumor neovasculature (25, 44). Hence, we rationalize that MT1-MMPs are available as a potential trigger for tumor-selective drug activation in a wide range of tumor types.

We designed and evaluated ICT2588, a COOH-terminal– and NH_2-terminal–modified peptide conjugate of the VDA azademethylcolchicine (ICT2552). ICT2588 possesses a peptide sequence rationalized to be specifically activated by MT1-MMP and was end-capped at its COOH terminus to prevent nonspecific exopeptidase degradation.

We showed conversion of ICT2588 to its active metabolite ($ICT2552^{act}$) and differential *in vitro* chemosensitivity in HT1080 (high MT1-MMP) but not in MCF7 (undetectable MT1-MMP) tumor cells. MMP dependency was shown by the lack of ICT2588 activation in the presence of the pan-MMP inhibitor ilomastat. In addition, MMP selectivity was supported by the cleavage of ICT2588 at the glycine-homophenylalanine bond by MT-MMPs but not by secreted MMPs. Although activation by MMP-2 was also evident at the P1′–P2′ position (homophenylalanine-tyrosine), this endopeptidase is not a major contributor to ICT2588 activation because hydrolysis was not significantly diminished by an MMP-2–selective inhibitor (CTT). Furthermore, MMP-2 activation is dependent on MT1-MMP activity (42).

This therapeutic strategy relies on specific MT-MMP activation of ICT2588 followed by subsequent nonspecific exopeptidase cleavage to produce azademethylcolchicine (ICT2552), the active VDA. In our analyses of tumor metabolism of ICT2588 *in vivo* and *ex vivo*, we observed only $ICT2552^{act}$ and no peptide-fragment metabolites of ICT2552. We interpret this to infer that MT-MMP cleavage of ICT2588 is followed by rapid exopeptidase-mediated degradation of the consequent $ICT2552^{act}$-peptide fragments to produce $ICT2552^{act}$.

Previous attempts to produce a MMP-activated peptide-conjugate of a chemotherapeutic were unable to produce agents that were sufficiently stable or tumor-selective *in vivo* (31). However, our study showed the stability of ICT2588 (peptide-conjugated VDA) in plasma and liver relative to rapid production of the active VDA ($ICT2552^{act}$) in tumor *ex vivo*, a finding confirmed by widespread distribution and stability of the nontoxic ICT2588 *in vivo* coupled to tumor-specific activation to $ICT2552^{act}$. Accumulation of ICT2588 and $ICT2552^{act}$ in the tumor may be due to the induction of vascular collapse and trapping of ICT2588 in the tumor microenvironment facilitating the prolonged availability of ICT2588 for metabolism by the MT1-MMP–dependent angiogenic tumor neovasculature.

Formation of active VDA in the tumors *in vivo* is consistent with the several-fold decrease in functional tumor vasculature and increased hemorrhagic necrosis, an observation consistent with the pharmacodynamics of other colchicine-like VDAs, such as ZD6126 and the combretastatins (2). Although equimolar doses of ICT2588 and ICT2552 caused comparative vascular shutdown, the magnitude of this effect was not consistent with their respective antitumor activities. Specifically, ICT2588 (75 mg/kg) produced a significant 2-fold greater growth delay (4.4 d; $P < 0.01$) compared with an equimolar dose of ICT2552 (15 mg/kg; 1.9 d). Furthermore, despite both the peptide-conjugated agent (ICT2588) and its authentic metabolite (ICT2552) demonstrating dose-response relationships, a significantly greater response was observed with equimolar equivalents of ICT2588. The superior efficacy of ICT2588 is likely due to the improved tumor-directed delivery and thus increased and prolonged tumor concentration of active VDA (ICT2552) in the peptide-conjugated form compared with the widely distributed and systemically active ICT2552.

Although monotherapy with ICT2588 resulted in a significant antitumor effect, a viable rim of tumor cells remained following treatment. The presence of this viable rim is consistent with previous reports following VDA treatment (1, 2) and is believed to be the result of these tumor cells receiving their nutrients and oxygen from the established vasculature of the surrounding normal tissues rather than the VDA-sensitive tumor vasculature (4). Consequently, the viable rim can be targeted by cotreatment with antiproliferative agents (2). In support of this, the combination of ICT2588 with doxorubicin resulted in a significant antitumor response, and more importantly, tumor cures in the majority of mice. The combination of ICT2588 and doxorubicin was superior to monotherapy irrespective of dosing and sequence schedule. The increased antitumor benefit of cotreatment with doxorubicin, 24 hours after ICT2588, is likely a result of doxorubicin targeting the proliferative cells in the viable rim, which are nonresponsive to ICT2588, and the ICT2588-mediated elimination of poorly perfused tumor areas, which are likely to be inaccessible or resistant to doxorubicin (45, 46). Mobilization of circulating endothelial cells into this region might also contribute to antitumor benefit, as suggested for ZD6126 and paclitaxel (45).

Clinical studies show that VDAs could demonstrate efficacy below their maximum tolerated doses; an observation consistent with ICT2588. This was the case with ICT2588 and doxorubicin in our study, suggesting that additive toxicity would be unlikely. The cardiovascular toxicity associated with several VDAs in clinical trials (5–7) is unlikely with ICT2588 because the circulating and cardiac levels of the active agent (ICT2552) are undetectable. This suggests a greater therapeutic index for ICT2588 relative to

Published OnlineFirst July 27, 2010; DOI: 10.1158/0008-5472.CAN-10-1440

other VDAs due to the tumor-selective release and elevated tumor concentrations of ICT2552^{act}, and the potential for reduced off-target toxicities. In conclusion, the significant therapeutic efficacy, *in vivo* stability, mechanism of action, tumor-selective release, and potential for circumventing systemic toxicity associated with systemically active VDAs strongly support ICT2588 as a potential therapeutic for the clinic.

Disclosure of Potential Conflicts of Interest

No potential conflicts of interest were disclosed.

Acknowledgments

We thank Patricia Cooper for *in vivo* studies.

Grant Support

This work at the Institute of Cancer Therapeutics was supported by programme grants from Cancer Research-UK and Yorkshire Cancer Research. The work by D.R. Edwards and C.J. Pennington was supported by a Cancer Research-UK project grant.

The costs of publication of this article were defrayed in part by the payment of page charges. This article must therefore be hereby marked *advertisement* in accordance with 18 U.S.C. Section 1734 solely to indicate this fact.

Received 04/27/2010; revised 07/13/2010; accepted 07/13/2010; published OnlineFirst 07/27/2010.

References

1. Lippert JW III. Vascular disrupting agents. Bioorg Med Chem 2007;15:605–15.
2. Kanthou C, Tozer GM. Microtubule depolymerizing vascular disrupting agents: novel therapeutic agents for oncology and other pathologies. Int J Exp Pathol 2009;90:284–94.
3. Davis PD, Dougherty GJ, Blakey DC, et al. ZD6126: a novel vascular-targeting agent that causes selective destruction of tumor vasculature. Cancer Res 2002;62:7247–53.
4. Tozer GM, Kanthou C, Baguley BC. Disrupting tumour blood vessels. Nat Rev Cancer 2005;5:423–35.
5. Hinnen P, Eskens FA. Vascular disrupting agents in clinical development. Br J Cancer 2007;96:1159–65.
6. van Heeckeren WJ, Bhakta S, Ortiz J, et al. Promise of new vascular-disrupting agents balanced with cardiac toxicity: is it time for oncologists to get to know their cardiologists? J Clin Oncol 2006;24:1485–8.
7. Cooney MM, Radivoyevitch T, Dowlati A, et al. Cardiovascular safety profile of combretastatin a4 phosphate in a single-dose phase I study in patients with advanced cancer. Clin Cancer Res 2004;10:96–100.
8. Deryugina EI, Quigley JP. Matrix metalloproteinases and tumor metastasis. Cancer Metastasis Rev 2006;25:9–34.
9. Egeblad M, Werb Z. New functions for the matrix metalloproteinases in cancer progression. Nat Rev Cancer 2002;2:161–74.
10. Overall CM, Kleifeld O. Tumour microenvironment—opinion: validating matrix metalloproteinases as drug targets and anti-targets for cancer therapy. Nat Rev Cancer 2006;6:227–39.
11. Abraham R, Schafer J, Rothe M, Bange J, Knyazev P, Ullrich A. Identification of MMP-15 as an anti-apoptotic factor in cancer cells. J Biol Chem 2005;280:34123–32.
12. Genis L, Galvez BG, Gonzalo P, Arroyo AG. MT1-MMP: universal or particular player in angiogenesis? Cancer Metastasis Rev 2006;25:77–86.
13. Plaisier M, Kapiteijn K, Koolwijk P, et al. Involvement of membrane-type matrix metalloproteinases (MT-MMPs) in capillary tube formation by human endometrial microvascular endothelial cells: role of MT3-MMP. J Clin Endocrinol Metab 2004;89:5828–36.
14. Sounni NE, Noel A. Membrane type-matrix metalloproteinases and tumor progression. Biochimie 2005;87:329–42.
15. Yana I, Seiki M. MT-MMPs play pivotal roles in cancer dissemination. Clin Exp Metastasis 2002;19:209–15.
16. Seiki M. Membrane-type 1 matrix metalloproteinase: a key enzyme for tumor invasion. Cancer Lett 2003;194:1–11.
17. Strongin AY. Proteolytic and non-proteolytic roles of membrane type-1 matrix metalloproteinase in malignancy. Biochim Biophys Acta 2010;1803:133–41.
18. Szabova L, Chrysovergis K, Yamada SS, Holmbeck K. MT1-MMP is required for efficient tumor dissemination in experimental metastatic disease. Oncogene 2008;27:3274–81.
19. Soulie P, Carrozzino F, Pepper MS, Strongin AY, Poupon MF, Montesano R. Membrane-type-1 matrix metalloproteinase confers tumorigenicity on nonmalignant epithelial cells. Oncogene 2005;24:1689–97.
20. Zhang W, Matrisian LM, Holmbeck K, Vick CC, Rosenthal EL. Fibroblast-derived MT1-MMP promotes tumor progression *in vitro* and *in vivo*. BMC Cancer 2006;6:52.
21. Rutkauskaite E, Volkmer D, Shigeyama Y, et al. Retroviral gene transfer of an antisense construct against membrane type 1 matrix metalloproteinase reduces the invasiveness of rheumatoid arthritis synovial fibroblasts. Arthritis Rheum 2005;52:2010–4.
22. Sabeh F, Ota I, Holmbeck K, et al. Tumor cell traffic through the extracellular matrix is controlled by the membrane-anchored collagenase MT1-MMP. J Cell Biol 2004;167:769–81.
23. Ueda J, Kajita M, Suenaga N, Fujii K, Seiki M. Sequence-specific silencing of MT1-MMP expression suppresses tumor cell migration and invasion: importance of MT1-MMP as a therapeutic target for invasive tumors. Oncogene 2003;22:8716–22.
24. Handsley MM, Edwards DR. Metalloproteinases and their inhibitors in tumor angiogenesis. Int J Cancer 2005;115:849–60.
25. Devy L, Huang L, Naa L, et al. Selective inhibition of matrix metalloproteinase-14 blocks tumor growth, invasion, and angiogenesis. Cancer Res 2009;69:1517–26.
26. Sounni NE, Devy L, Hajitou A, et al. MT1-MMP expression promotes tumor growth and angiogenesis through an up-regulation of vascular endothelial growth factor expression. FASEB J 2002;16:555–64.
27. Rautio J, Kumpulainen H, Heimbach T, et al. Prodrugs: design and clinical applications. Nat Rev Drug Discov 2008;7:255–70.
28. Patterson LH. Bioreductively activated antitumor N-oxides: the case of AQ4N, a unique approach to hypoxia-activated cancer chemotherapy. Drug Metab Rev 2002;34:581–92.
29. Albertella MR, Loadman PM, Jones PH, et al. Hypoxia-selective targeting by the bioreductive prodrug AQ4N in patients with solid tumors: results of a phase I study. Clin Cancer Res 2008;14:1096–104.
30. Walko CM, Lindley C. Capecitabine: a review. Clin Ther 2005;27:23–44.
31. Atkinson JM, Siller CS, Gill JH. Tumour endoproteases: the cutting edge of cancer drug delivery? Br J Pharmacol 2008;153:1344–52.
32. Workman P, Twentyman P, Balkwill F, et al. United Kingdom Co-Ordinating Committee on Cancer Research (UKCCCR) guidelines for the welfare of animals in experimental neoplasia (second edition). Br J Cancer 1998;77:1–10.
33. Atkinson JM, Pennington CJ, Martin SW, et al. Membrane type matrix metalloproteinases (MMPs) show differential expression in non-small cell lung cancer (NSCLC) compared to normal lung: correlation of MMP-14 mRNA expression and proteolytic activity. Eur J Cancer 2007;43:1764–71.
34. Nuttall RK, Pennington CJ, Taplin J, et al. Elevated membrane-type matrix metalloproteinases in gliomas revealed by profiling proteases and inhibitors in human cancer cells. Mol Cancer Res 2003;1:333–45.

Published OnlineFirst July 27, 2010; DOI: 10.1158/0008-5472.CAN-10-1440

35. Gill JH, Loadman P, Falconer RA, Patterson LH, Atkinson JM, Bibby MC inventors; University of Bradford, applicant. MMP activated vascular disrupting agents. UK patent WO2008125800. 2008 October 23.
36. Mosmann T. Rapid colorimetric assay for cellular growth and survival: application to proliferation and cytotoxicity assays. J Immunol Methods 1983;65:55–63.
37. Shnyder SD, Cooper PA, Millington NJ, Pettit GR, Bibby MC. Auristatin PYE, a novel synthetic derivative of dolastatin 10, is highly effective in human colon tumour models. Int J Oncol 2007;31:353–60.
38. Yamamoto M, Tsujishita H, Hori N, et al. Inhibition of membrane-type 1 matrix metalloproteinase by hydroxamate inhibitors: an examination of the subsite pocket. J Med Chem 1998;41:1209–17.
39. Koivunen E, Arap W, Valtanen H, et al. Tumor targeting with a selective gelatinase inhibitor. Nat Biotechnol 1999;17:768–74.
40. Quinn PK, Bibby MC, Cox JA, Crawford SM. The influence of hydralazine on the vasculature, blood perfusion and chemosensitivity of MAC tumours. Br J Cancer 1992;66:323–30.
41. Smith KA, Hill SA, Begg AC, Denekamp J. Validation of the fluorescent dye Hoechst 33342 as a vascular space marker in tumours. Br J Cancer 1988;57:247–53.
42. Ingvarsen S, Madsen DH, Hillig T, et al. Dimerization of endogenous MT1-MMP is a regulatory step in the activation of the 72-kDa gelatinase MMP-2 on fibroblasts and fibrosarcoma cells. Biol Chem 2008;389:943–53.
43. Drew AF, Blick TJ, Lafleur MA, et al. Correlation of tumor- and stromal-derived MT1-MMP expression with progression of human ovarian tumors in SCID mice. Gynecol Oncol 2004;95:437–48.
44. Yana I, Sagara H, Takaki S, et al. Crosstalk between neovessels and mural cells directs the site-specific expression of MT1-MMP to endothelial tip cells. J Cell Sci 2007;120:1607–14.
45. Martinelli M, Bonezzi K, Riccardi E, et al. Sequence dependent antitumour efficacy of the vascular disrupting agent ZD6126 in combination with paclitaxel. Br J Cancer 2007;97:888–94.
46. Evans CJ, Phillips RM, Jones PF, et al. A mathematical model of doxorubicin penetration through multicellular layers. J Theor Biol 2009;25:598–608.

AACR American Association for Cancer Research

Cancer Research

The Journal of Cancer Research (1916–1930) | The American Journal of Cancer (1931–1940)

Development of a Novel Tumor-Targeted Vascular Disrupting Agent Activated by Membrane-Type Matrix Metalloproteinases

Jennifer M. Atkinson, Robert A. Falconer, Dylan R. Edwards, et al.

Cancer Res 2010;70:6902-6912. Published OnlineFirst July 27, 2010.